

Original Research Article

Corrosion Inhibition Potential of Benue Propolis Extracts on Carbon Steel in 1.0 M Hydrochloric Acid Medium: Experimental and Computational Studies

A. M. Orokpo*, R. A. Wuana, H.F. Chuhul, I.S. Eneji

Department of Chemistry, Federal University of Agriculture, PMB, 2373, Makurdi, Nigeria

ARTICLE INFO

Article history

Submitted: 2022-08-05

Revised: 2022-09-09

Accepted: 2022-09-25

Available online: 2022-09-29

Manuscript ID: PCBR-2208-1231

DOI: 10.22034/pcbr.2022.354920.1231

KEYWORDS

Propolis

Cycloeucaenol

Carbon steel

Corrosion Inhibition

Adsorption

Density Functional Theory (DFT)

ABSTRACT

Cycloeucaenol (CEU) was the major composition of the Benue Propolis extracts identified via proton NMR. The corrosion inhibition behaviour of this extracts on carbon steel in 1.0 M HCl was investigated by using weight loss, electrochemical impedance spectroscopy, and computational methods. The results obtained revealed that the inhibition efficiency increased with an increase in inhibitor concentration, but decreased with increase in temperature. Impedance measurement showed that charge transfer was responsible for the corrosion process. The charge transfer resistance (R_2) increased with concentration of the inhibitor as opposed to the double layer capacitance (Cdl) which decreased. The values of the Gibbs free energy (ΔG°) indicated a spontaneous adsorption of the extract components on the metal surface. The physically adsorbed propolis extract onto the carbon steel surface followed Langmuir adsorption isotherm model. The HOMO map shows the electron cloud situated in the C=C sp^2 group, and then spread across the three consecutive cyclohexane rings and their substituents. From the Fukui function indices calculations, CEU is discovered to have its site for nucleophilic and electrophilic attacks each at one of carbon atoms of the alkene group in the molecule. The results have demonstrated that the composition of Benue propolis is active inhibitor of corrosion of carbon steel surface in HCl acidic medium.

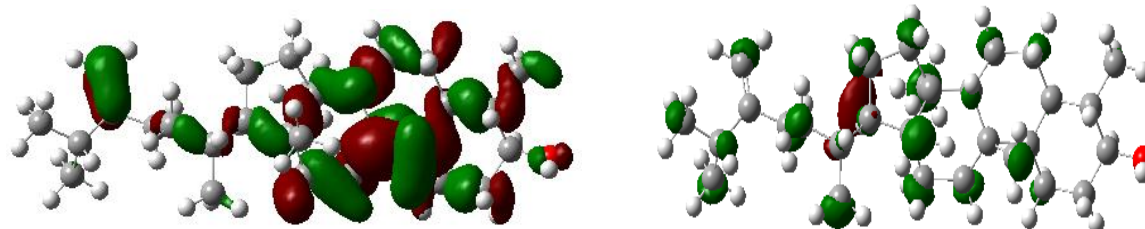
* Corresponding author: Apeh Michael Orokpo

✉ E-mail: orokpoapeh@gmail.com

© 2022 by SPC (Sami Publishing Company)



GRAPHICAL ABSTRACT



1. Introduction

Corrosion is a highly destructive naturally occurring phenomenon affecting the performance of metallic materials in application, especially carbon steel. Carbon steel is most predominantly used for both industrial and domestic purposes, thus, most affected by corrosion [1]. Incurring of humongous losses associated with this irreversible deterioration of metals, in general, and carbon steel, in particular, necessitates preventive measures. The use of inhibitor has been proven to be one of the most effective, economical, and eco-friendly method of preventing and controlling corrosion [2].

As in 2013, equivalent to 3.4% of the global GDP amounting to \$2.5 trillion was estimated as the global cost of corrosion. In Nigeria alone, oil and gas industry lose average of \$765 million to corrosion annually. Of this amount, chemical treatment gulps 81% of the entire cost, while coating takes the balanced 19% cost of prevention. With respect to the contribution of corrosion maintenance methods, 60% goes for repairs while 40% for replacement. About 35% of the corrosion cost is estimated to be a realizable savings on a global basis if available corrosion control practices are applied, this amounts to \$875 billion, [3-4]. The application of

organic corrosion inhibitors like propolis extract will contribute greatly to minimize losses due to corrosion.

Also called bee glue, propolis is a resinous substance prepared by honeybees from flowers and leaf buds to seal the cracks, smooth walls, to keep moisture content and temperature stable as well as maintain the hive environment aseptic all year around. It consists of a mixture of pollen, waxes, essential and aromatic oils, and other organic substances including enzymes secreted by bees. In recent years, propolis have attracted the interest of researchers due to its broad spectrum of biological properties vizantimicrobial, antioxidant anti-inflammatory, antitumor, antiulcer, anti-HIV, and antiulcer activities [5]. It is widely used to prevent and treat cold, wounds and ulcers, rheumatism, sprains, heart disease, diabetes, and dental caries. The colour and chemical composition of propolis varies depending on the plants from where the materials are collected, the season of collection, the location of the hive, the breeds of bees, and the time at which it was made [6-8].

After extracting honey, the squeezed honeycomb which contains propolis is thrashed and becomes an organic waste with no market value. However, the honeycomb waste still contains relatively

high flavonoids. These organic flavonoids structures contain electronegative atom, conjugated double bonds, or aromatic rings that can be exploited as a corrosion inhibitor [9] in this research.

2. Experimental

2.1. Materials and Methods

2.1.1. Materials

Mortar and pestle, desiccator, NMR machine, Fourier Transform Infrared Spectrophotometer (FTIR), digital weighing balance, thermostated water bath, and potentiostat are some of the materials used. Other materials include carbon steel, bristle brush, and silicon carbide abrasive paper (#600-#1200). Also used are two necked reaction flask, thermometer, measuring cylinders, beakers, and routine laboratory apparatus. The reagents were of analar grade with re-distillation of the solvents; n-hexane, ethyl acetate, and methanol. Hydrochloric acid solution was used as aggressive environment, acetone as drying agent, sodium hydroxide, and ethanol for cleaning and degrease, respectively. The preparation of the reagents was carried out by using double distilled water.

2.1.2. Preparation and extraction of propolis samples

Propolis samples were bought from bee farmer in Benue State, Nigeria. The propolis samples were air dried for two weeks, and then pounded with a pestle and mortar. The fine powdered samples (100 g) were initially defatted with n-hexane at room temperature by macerating for 72 hours. This was followed by filtration with Whitman filter paper No. 1 by using a vacuum pump. Following the same procedure, the residues were re-extracted with ethyl acetate and methanol, respectively. The solvents were completely removed by using a rotary vacuum evaporator. The powdery extracts were then kept in dark bottles at 4 °C until use. From a portion of the concentrated extract, column

chromatography and TLC was carried out to further separate and purify the extracts for the NMR analysis.

2.1.3. ¹H NMR Analysis of the Propolis Extracts

Nuclear Magnetic Resonance (NMR) spectroscopic analysis on fractions of the propolis were analysed by using a Bruker-Avance 400 MHz) spectrophotometer with deuterated chloroform as solvent. The NMR data were analysed by using Mestrenova 12 software. Characterization and structure elucidation of the compounds was based on their ¹H compared with some selected literatures

2.3. Corrosion Inhibition Experiments

2.3.1. Gravimetric measurement

To study the effect of concentration of the propolis extract on corrosion of carbon steel, pre-cleaned and pre-weighed carbon steel coupons were immersed for 24 hours in 1.0 M HCl. This was carried out in the absence and presence of 200-1000 ppm propolis extract at room temperature. The weight loss was taken to be the difference in weights of the coupon taken before and after the period of immersion. To determine the effect of time on the corrosion rate of the carbon steel, the coupons were retrieved at specific interval (24, 48, 72, 96, 120, 144, and 168 hours) at room temperature after which they were cleaned with distilled water, acetone, dried, and re-weighed.

To investigate the temperature effect, the test was carried out at 303, 313, 323, and 333 K, respectively for 3 hours of immersion in the absence and presence of the various concentrations of the propolis extract. The weight loss was also taken to be the difference between the initial weights and the final weight of the coupon after 3 hours. All tests were carried out in duplicate. From the weight loss results, the inhibition efficiency (%IE) of the inhibitor and corrosion rate of carbon steel was calculated by using Equations 1-2 [10].

$$IE_{\text{exp}} = \left(1 - \frac{W_{(1)}}{W_{(0)}}\right) \times 100 \quad 1$$

Where, $W_{(0)}$ is the weight loss of the carbon steel without inhibitor and $W_{(1)}$ is the weight loss of carbon steel with inhibitor.

$$CR(\text{gh}^{-1}\text{cm}^{-2}) = \frac{\Delta W}{At} \quad 2$$

Where, ΔW is the weight loss, A is the area of the coupon, and t is the immersion time.

2.3. Electrochemical Impedance Spectroscopy (EIS) measurements

The experiments were conducted at 303 K by using 200 mL of test solution. A conventional three-electrode system consisting of carbon steel as working electrode, an auxiliary electrode and a reference electrode were used for the measurements. The %IE was calculated from the charge transfer resistance (R_{ct}) values by using the following equation.

$$\%IE = \frac{R_{ct} - R_{ct}^0}{R_{ct}} \times 100 \quad 3$$

Where, R_{ct}^0 is the charge transfer resistance of MS without inhibitor and R_{ct} is the charge transfer resistance of MS with inhibitor. The double layer capacitance (C_{dl}) was calculated by using Equation 4.

$$C_{dl} = \frac{1}{2\pi f_{max} R_{ct}} \quad 4$$

Where, f_{max} is the frequency at which the imaginary component of impedance is the maximum

3. Quantum Chemical Calculation

Full geometric optimization was carried out by using ab initio and DFT level of theories in the HyperChem release 8.0 software. Semi-empirical parameters were calculated in different

Hamiltonians: CNDO, MNDO, and INDO: AM1 (Austin Model 1) and PM3 (Parametric Method 3), by using optimized structure of the studied inhibitor as an input to the software Windows. Calculations were performed on compatible laptop computer. The following quantum chemical indices were calculated: the Energy of the Highest Occupied Molecular Orbital (E_{HOMO}), the Energy of the Lowest Unoccupied Molecular Orbital (E_{LUMO}), the binding energy (E_b), the electronic energy (E_{elect}), the core repulsion energy E_{CCR} , the dipole moment (μ), the heat of formation (H_f), and the total energy of the molecule (E_T).

4. Results and Discussion

4.1.1. ^1H NMR Analysis

The ^1H NMR spectrum of the propolis sample is displayed as Figure 1 and the characteristic signals obtained from the spectrum are recorded as Table 1. The table presents 3.20 (m, H3), 4.64 (s, H28), and 4.70 (s, H28) as the most interesting information obtained from the spectrum. Compared the data with literature, *Cycloeucaleanol* (CEU) was the identifiable compound present in BPE, as depicted in Figure 2 [11].

Cycloeucaleanol is a cycloartane triterpene, a steroid containing a cycloartanol moiety which is an extremely weak basic (essentially neutral) compound based on its pKa. The ^1H NMR data compares well with that of Adewusia *et al.* [12]. As a terpenoid, its functional group, due to the heteroatom presence, is the active inhibitor of corrosion [13].

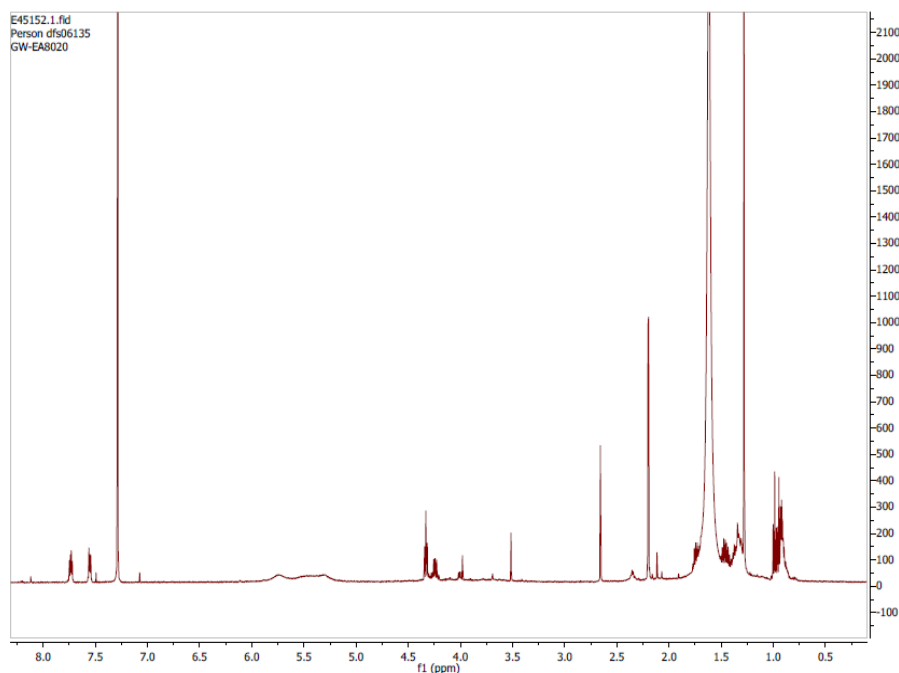


Fig. 1. Proton NMR spectrum of BPE

Table 1. ¹H-NMR data from BPE

Compounds	¹ H-NMR data δ (Multiplicity/Hz) selected from literature	¹ H-NMR data δ (Multiplicity/Hz) selected from experimental result
Cycloeucaleanol	3.20 (m, H3), 4.64 (s, H28), and 4.73 (s, H28).	3.20 (m, H3), 4.64 (s, H28), and 4.70 (s, H28).

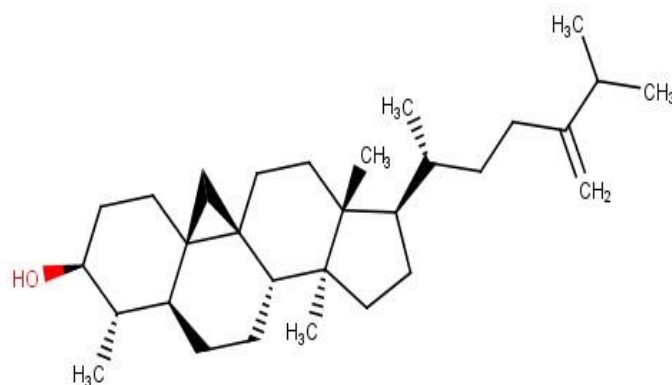


Fig. 2. Structure of *Cycloeucaleanol* elucidated from BPE

4.1.2. FTIR Study

The FTIR analysis of the BPE was carried out to ascertain the functional groups present in the

sample. **Figures 3** shows the spectrum of raw BPE and that of the corrosion product. The important peaks are recorded in **Table 2**.

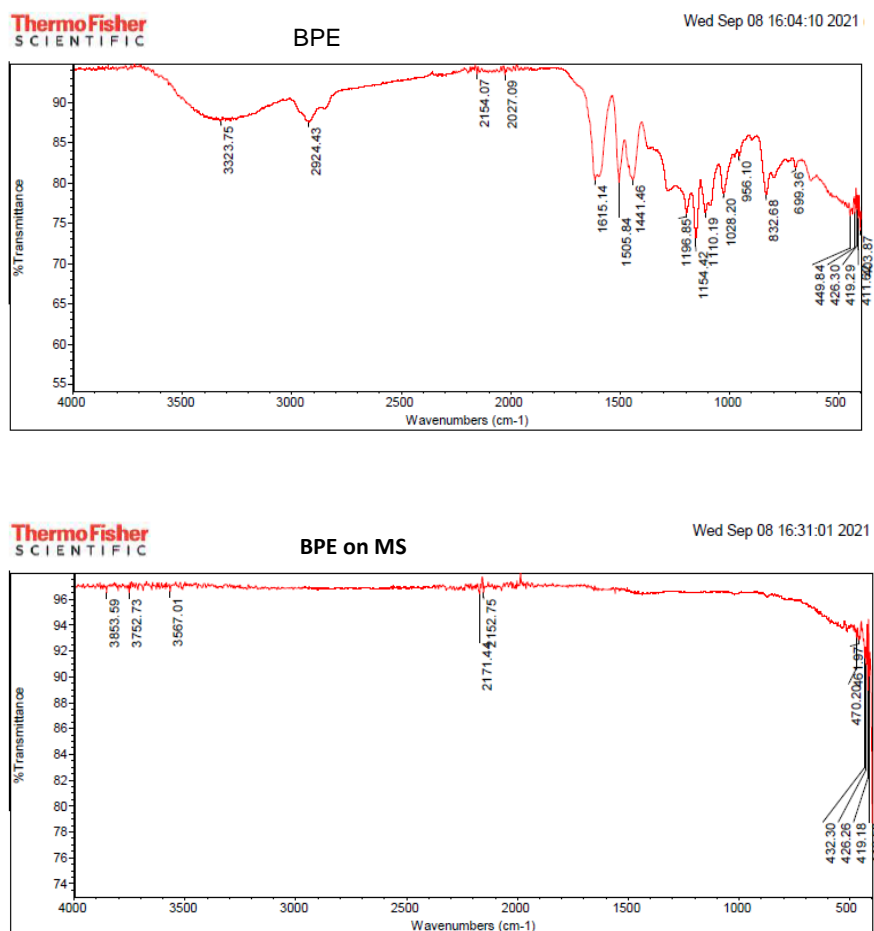


Fig. 3. FTIR spectrum of BPE and the corrosion product of the carbon steel in the presence of BPE

Table 2. Frequencies and peak intensities of FTIR absorption by BPE and the corrosion product of the carbon steel in the BPE presence

ENPE before adsorption		Corrosion product in the presence of ENPE		Functional group/assignment
Frequency (cm ⁻¹)	Intensity	Frequency (cm ⁻¹)	Intensity	
		3853.59	Weak	Alcohol
		3752.73	Weak	Alcohol
3323.68	Broad, strong	3567.01	Weak	O-H stretching
2924.43	Strong, sharp			O-H stretching
2154.07	Weak	2171.44	Weak	C-H stretching
2027.09	Weak	2152.75	Weak	C-H stretching
1615.14	Strong			C=O stretching
1505.84	Strong			C=C stretching
1441.46	Strong			N-O stretching
1196.85	Strong			O-H Alcohol
1154.42	Strong			O-H bending
1110.19	Medium			C-O stretching of tertiary alcohol
1028.20	Strong			C-N stretching
956.10	Weak			C-H bending
832.68	Strong			C-H stretching

The broad and strong intensities at peaks ranging from 3323.68 cm^{-1} to 2924.43 cm^{-1} are due to O-H group, 2154.07 cm^{-1} correspond to alkyl C-H stretching, 2027.09.12 cm^{-1} is assigned C-H stretching, 1615.14 cm^{-1} is attributed to C=O stretching, 1505.84 cm^{-1} is assigned C=C stretching, and the 1441.46 cm^{-1} is assigned N-O stretching. The peak at 1196.85 cm^{-1} is attributed to O-H stretching of alcohol, 1154.42 cm^{-1} is assigned O-H bending, while the peak at 1110.19 cm^{-1} corresponds to C-O stretching of tertiary alcohol. The peak at 1028.20 is assigned C-N stretching, while the peak ranging from 956.10 to 832.68 are assigned C-H stretching. It can be seen that functional groups not part of CEU was identified by the FTIR analysis. This implies the possibility of the compound's presence other than CEU in the used propolis sample.

4.2. Corrosion Inhibition Studies

4.2.1. Gravimetric Measurements

Table 3 present the inhibition efficiencies of BPE on carbon steel in 1.0 M HCl calculated from Equation 1. It can be seen from the results

obtained, the inhibition efficiencies increased with increase in the inhibitor concentration .

The corrosion rates obtained from the analysis in the absence and presence of BPE by using Equation 2 are shown in **Figure 4**. The corrosion rates were found to decrease with increase in concentration of BPE but increase with time. With reference to the values of inhibition efficiencies obtained at different concentration of BPE presented as Table 3, it can be seen that the inhibition efficiencies increased with increase in concentration of BPE. This behaviour could be attributed to the increase in adsorption of inhibitor on the metal or at the solution interface on increasing its concentration [14]. The corrosion rates obtained from the analysis in the absence and presence of BPE as indicated in Figure 4 were found to decrease with increase in the BPE concentration but increased with time.

Table 3. Inhibition efficiencies of the various inhibitors on carbon steel in 1.0 M HCl

Time (hours)	BPE Concentration (ppm)					
	Blank	200	400	600	800	1000
24	-	59.98	62.00	64.43	68.22	72.15
48	-	62.29	72.15	73.70	76.10	78.11
72	-	68.67	73.33	73.81	76.67	79.27
96	-	70.34	74.94	77.53	78.83	81.43
120	-	77.95	80.23	81.79	83.03	84.36
144	-	78.75	81.25	82.50	83.75	86.25
168	-	80.62	85.00	85.18	88.46	93.59

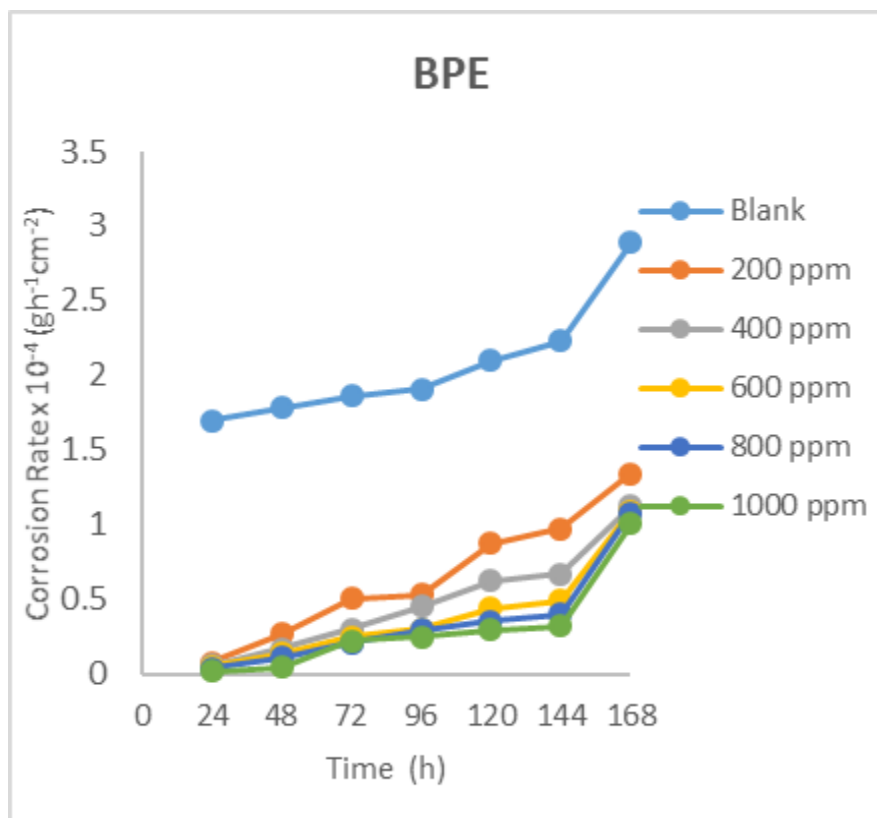


Fig. 4. Corrosion rates of carbon steel in 1.0 M HCl in the absence and presence of the various concentration of BPE as a function of immersion time (h)

4.2.2. Effect of Heat

The values of inhibition efficiencies of BPE on carbon steel in 1.0 M HCl based on effects of heat consideration measurements at 303, 313, 323, 333, and 343 K are summarized in Table 4. Inhibition efficiencies increase with increase in the BPE concentration, a trend similar to the results obtained with effects of time consideration, though with varied magnitude of the inhibition efficiencies, where results obtained from the effect of temperature are relatively lower than those obtained from effect of time measurements. However, the inhibition

efficiencies decreased with increase in temperature. Also, the corrosion rates, as shown in Figure 5, were found to increase with temperature. This is again evidence that BPE is the effective corrosion inhibitor for carbon steel in hydrochloric acid. The reduction in inhibition efficiency with increasing temperature is attributed to physical adsorption of BPE to the surface of the carbon steel. It has been reported that physical adsorption is favoured at lower temperature, whilst chemisorption is favoured at higher temperature [15].

Table 4. Inhibition Efficiencies of BPE on Carbon Steel in 1.0 M HCl at 303-343 K

Temperature (K)	BPE Concentration (ppm)					
	Blank	200	400	600	800	1000
303	-	55.67	60.34	74.42	81.00	89.13
313	-	51.32	57.52	58.88	71.02	77.08
323	-	49.54	55.66	55.10	60.07	63.37
333	-	30.23	31.87	40.03	49.61	53.37
343	-	27.60	32.17	34.66	37.99	41.44

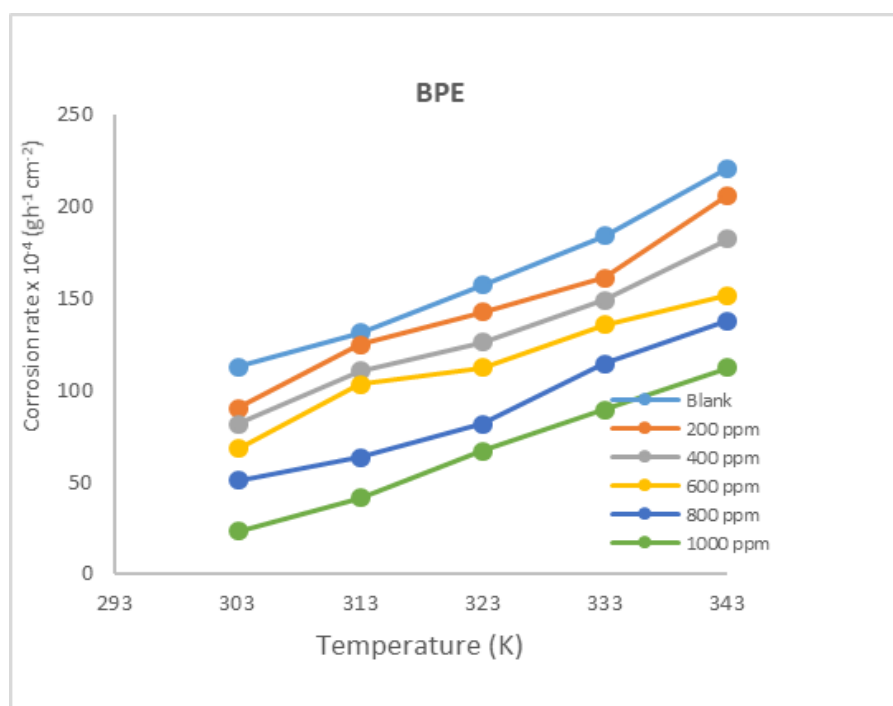


Fig. 5. Corrosion rates of carbon steel in 1.0 M HCl in the absence and presence of various concentrations of BPE as a function of temperature (K)

4.3. Electrochemical Measurements

Electrochemical Impedance Spectroscopy (EIS) measurements at the open-circuit potential were carried out to determine the kinetic parameters for electron transfer reactions at the steel/electrolyte interface and simultaneously regarding the surface properties of the investigated system. The best fit equivalent circuits were used to analyse the impedance data, based on the shapes of the Nyquist plots. A simplest Randles equivalent circuit as shown in **Figure 6** is used to fit the Nyquist plot in the absence and presence of inhibitor in 1.0 M hydrochloric acid solution. It consists of fast charge transfer process R_1 , the surface layer resistance R_2 , and one constant phase element (CPE). The polarisation resistance R_p , which is equivalent to charge transfer resistance R_{ct} was calculated by the summation of R_1 and R_2 at different concentrations of inhibitor and the resultant R_{ct} was used to calculate the percentage inhibition efficiency from Equation 3. Also, the

double layer capacitance (C_{dl}) was calculated from Equation 4. The parameters obtained from the measurement of EIS, as listed in Table 5, are the charge transfer resistance (R_{ct}), constant phase element (CPE) and inhibition efficiencies. The impedance diagram obtains yield a single depressed semicircle shape. This means that charge transfer is responsible for the corrosion process. The modulus of the Nyquist plots in 1.0 M HCl solution without the inhibitor was much smaller than that in the presence of the inhibitors. The Nyquist plot reveals that increasing the inhibitor concentration causes an increase in both the diameter of the semicircles and the R_{ct} values; this can be attributed to the increase in the number of absorbed inhibitor molecules on the surface of the carbon steel with increase in concentration. This also implies an increase in the corrosion inhibition efficiency, as can be seen in Table 5. From the ohmic law, where $V = iR$, the higher the resistance value (R_{ct}), the lower the electrical current (i) flow, the

lower the number of electrons transferred across the metal surface. Thus, cathodic oxidation of the carbon steel is inhibited. The similarity in the semicircles shape both in the absence and presence of the inhibitors indicates similar corrosion mechanism irrespective of the addition of the inhibitors. Thus, the addition of inhibitors has no significant influence on the corrosion mechanism of the carbon steel in 1.0 M HCl solution. The value of 'n' which is less than 1 is due to the surface heterogeneity [16]. The equivalent circuit depicted in Figure 6 is employed to analyse the impedance spectra, where R_1 represents the solution resistance, R_2 denotes the charge-transfer resistance, and a CPE instead of a pure capacitor represents the interfacial capacitance. The Nyquist diagrams (Figure 7) are not perfect semicircles, a phenomenon that is referred to as the frequency dispersion of interfacial impedance. This is due

to the surface roughness or inhomogeneity of the metal surface associated with solid metal electrodes because of the presence of a non-ideal frequency response for which constant phase element CPE was used [17].

Figures 8 (A and B) shows the Bode impedance and Bode phase plots obtained for the carbon steel electrode in the absence and in the presence of BPE in 1.0 M HCl solution. It can be seen that the Bode plot consist of a one loop capacitive. From the Bode phase plot, it can be observed that increase in the inhibitor concentration caused more negative values of phase angle at the intermediate frequency. As the inhibitor's concentration increased, the values of phase angle become more negative. This indicates that the inhibitive behaviour occurred because more of the inhibitor molecules are adsorbed at the carbon steel surface [18].

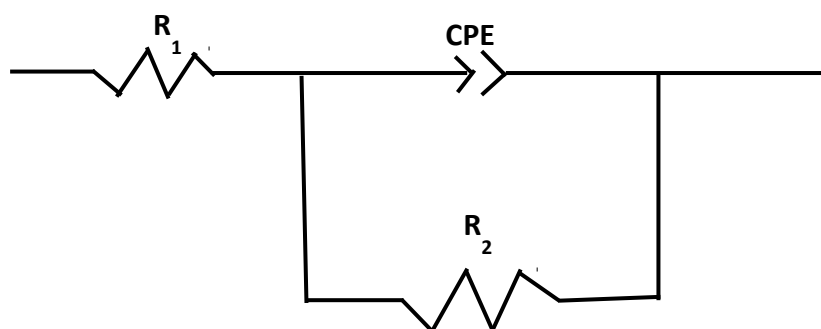


Fig. 6. Equivalent circuits used to fit experimental EIS data for the corrosion of the carbon steel in 1.0 M hydrochloric acid solution in the absence and presence of the inhibitor

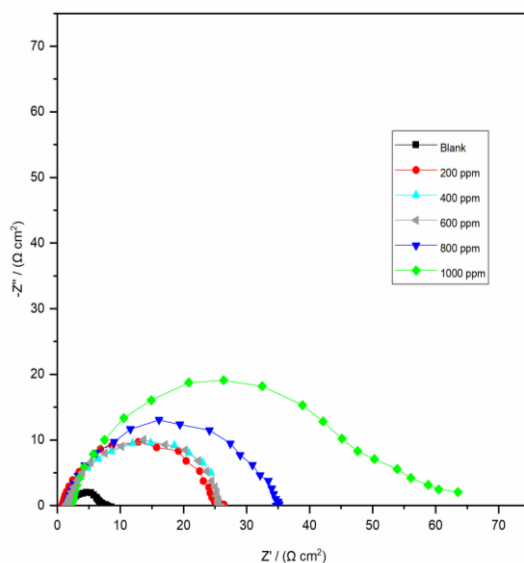


Fig. 7. Nyquist plots for the carbon steel specimen in 1.0 M HCl in the absence and presence of different concentrations of BPE

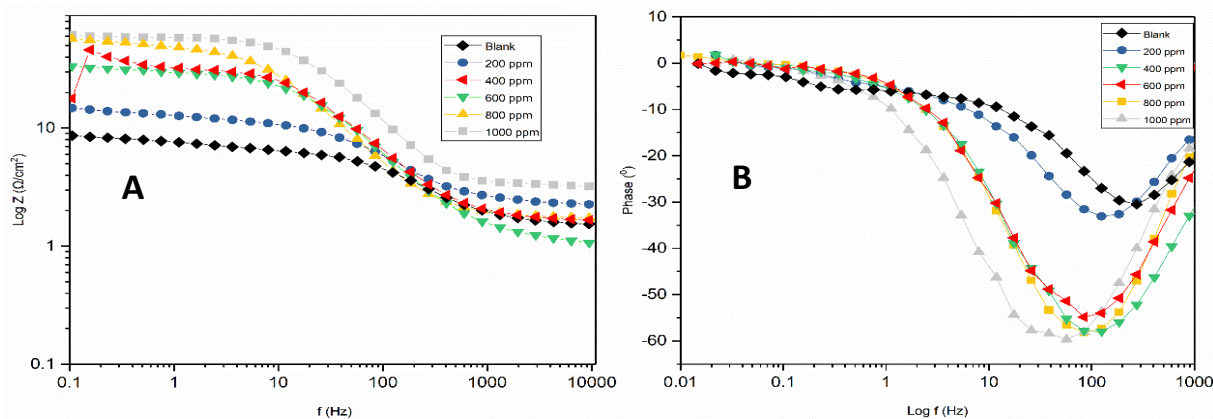


Fig. 8. (A) Bode impedance and (B) Bode phase plots for carbon steel electrode in the absence presence of BPE in 1.0 M HCl

Table 5. Impedance parameters for the corrosion of carbon steel in 1.0 M HCl in the absence and presence of various concentrations of the inhibitors

Concentration (ppm)	R_1 (Ω cm ²)	R_2 (Ω cm ²)	R_{ct} (Ω cm ²)	C_{dl} (μ F cm ⁻²)	N	%IE
Blank	1.205	10.414	11.619	9.34×10^{-4}	0.88	-
200	2.302	21.279	23.581	5.93×10^{-4}	0.92	50.73
400	1.528	29.779	31.307	1.32×10^{-4}	0.91	62.89
600	1.030	32.544	33.574	1.18×10^{-4}	0.89	65.39
800	1.656	49.213	50.869	6.30×10^{-5}	0.89	77.16
1000	1.764	63.823	65.587	2.50×10^{-5}	0.95	82.28

4.4. Thermodynamic Consideration

The thermodynamic behaviour of BPE was critically studied to gain insight into the inhibition mechanism of the corrosion of carbon

steel in 1.0 M HCl by BPE. Thermodynamic parameters such as the energy of activation (E_a), standard enthalpy (ΔH), and the entropy changes of adsorption (ΔS) were deduced through the

transition state plots. The transition state Equation 5 relates the corrosion rate with these thermodynamic parameters, which was further resolved to a linear expression of Equation 6.

$$CR = \frac{RT}{Nh} \exp\left(\frac{\Delta S_{ads}}{R}\right) \exp\left(\frac{-\Delta H_{ads}}{RT}\right) \quad 5$$

$$\log\left(\frac{CR}{T}\right) = \log\left(\frac{R}{Nh}\right) + \left(\frac{\Delta S_{ads}}{2.303R}\right) - \left(\frac{\Delta H_{ads}}{2.303RT}\right) \quad 6$$

Figure 9a demonstrates the Arrhenius plot for the corrosion of carbon steel in 1.0 M HCl containing the various concentration of the BPE. The parameters deduced are recorded as Table 6. Accordingly, it can be seen that the values for the activation energy in the BPE presence are higher than in the blank. The Ea values also increased with increase in the inhibitor concentration. The Ea obtained for corrosion of carbon steel in blank 1.0 M HCl was found to be 14.68 Jmol⁻¹ and increased with increasing concentration of the inhibitor, with the highest values of 34.41 Jmol⁻¹, in the presence of 1000 ppm BPE. This showed that the adsorbed inhibitor has provided a physical barrier to the change and mass transfer, leading to reduction in corrosion rate [19]. It has been reported earlier that the Ea value greater than 80 kJ mol⁻¹ indicates chemical adsorption,

while Ea less than 80 kJ mol⁻¹ infers physical adsorption [20]. From the experimentally determined Ea values which are all less than 80 kJ mol⁻¹, it is evidenced that BPE was physically adsorbed on the coupons. Therefore, it is plausible that a multilayer protective coverage on the entire carbon steel surface was obtained. The transition state plots for the corrosion of carbon steel in 1.0 M HCl in the absence and in the presence of BPE are displayed as Figure 9b. The corresponding transition state parameters such as ΔH and ΔS obtained from the plot of $\ln\left(\frac{CR}{T}\right)$ vs $\frac{1}{T}$ are recorded in Table 6. As can be seen from the table, the ΔS values are negative and decreased progressively with increase in the inhibitor concentration, indicating that the inhibitor molecules freely moving in the bulk solution were adsorbed in an orderly fashion onto the carbon steel surface. This implies that the activation complex represents association steps and that the reaction was spontaneous and feasible. Also, results showed that all the ΔH for the inhibitors are negative, reflecting the exothermic nature of the carbon steel dissolution process [21].

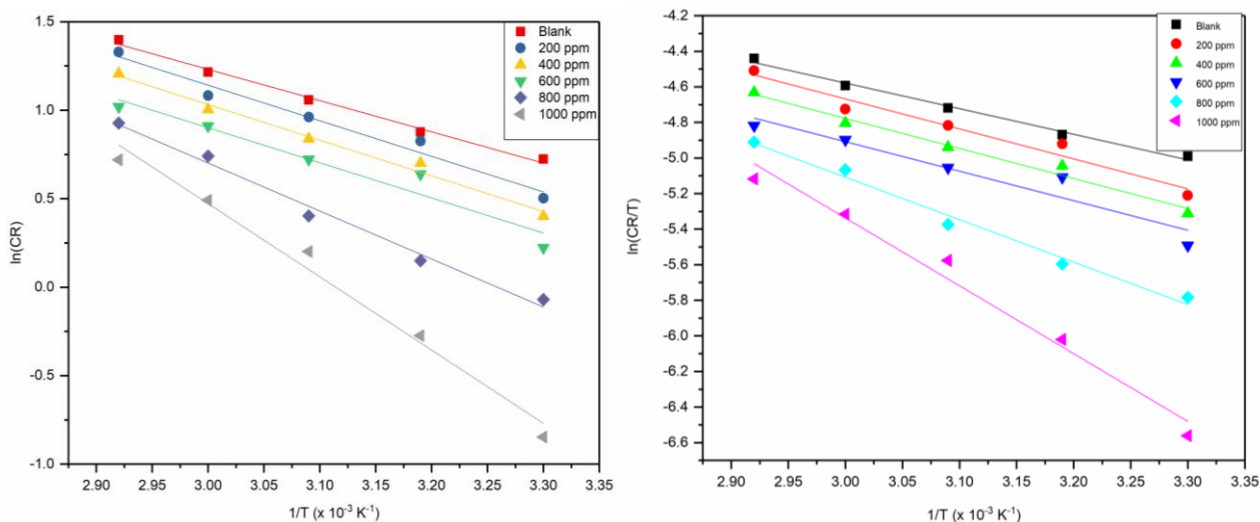


Fig. 9. (A) Arrhenius and (B) Transition state plot for the corrosion of carbon steel in 1.0 M HCl containing the various concentration of BPE

Table 6. (A) Arrhenius and **(B)** Transition state parameters for the corrosion of carbon steel in 1.0 M HCl containing various concentration of BPE

Concentration (ppm)	Ea (J/mol)	ΔS_{ads}^0 (J/mol)	ΔH_{ads}^0 (J/mol)	R ²
Blank	14.68	-199.68	-11.97	0.99
200	16.50	-194.31	-14.02	0.96
400	16.72	-195.11	-14.05	0.98
600	16.75	-96.97	-14.79	0.92
800	22.54	-180.49	-19.84	0.99
1000	34.41	-146.79	-31.72	0.98

4.5. Adsorption Consideration

Adsorption isotherm values are important to explain the mechanism of corrosion inhibition of organo-electrochemical reactions of metals and alloys. Equation 7 indicates the general form of adsorption isotherms. Different adsorption isotherms were tested to obtain more information about the interaction between the carbon steel surface and BPE at various temperatures. The different isotherms tested includes Temkin, Frumkin, Freundlich, Flory-Huggins, and Langmuir adsorption isotherms among others. The linear regression coefficients (R²) were used to determine the best fit. Langmuir adsorption isotherm was found to be best fit in which case the linear regression coefficients (R²) was close to unity. Langmuir adsorption isotherm assumes that the solid surface contains a fixed number of adsorption sites and each site holds one adsorbed species [22].

$$f(\theta, x) \exp^{-2a\theta} = KC \quad 7$$

The Langmuir isotherm plots of log C/θ against log C for the adsorption of BPE at various temperatures is shown as Figure 10. The equilibrium constant of adsorption of the inhibitors on the carbon steel surface is related to the standard free energy of adsorption ΔG_{ads}^0 by the following Equation:

$$\Delta G_{ads}^0 = -2.303RT \log (55.5K_{ads}) \quad 8$$

Where R is the molar gas constant, T is the absolute temperature, and 55.5 is the water concentration in solution expressed in mol L⁻¹. Langmuir parameters for the corrosion of carbon steel in 1.0 HCl containing various concentrations of BPE calculated from the slope and intercept of the plots are presented in Table 6. All the values obtained for in the ΔG were negative indicating that the adsorption process proceeded spontaneously and confirms physical adsorption mechanism. Generally, the value of $\Delta G_{ads}^0 \leq -40$ kJ mol⁻¹ signify physisorption and values more negative than -40 kJ mol⁻¹ signify chemisorption [23].

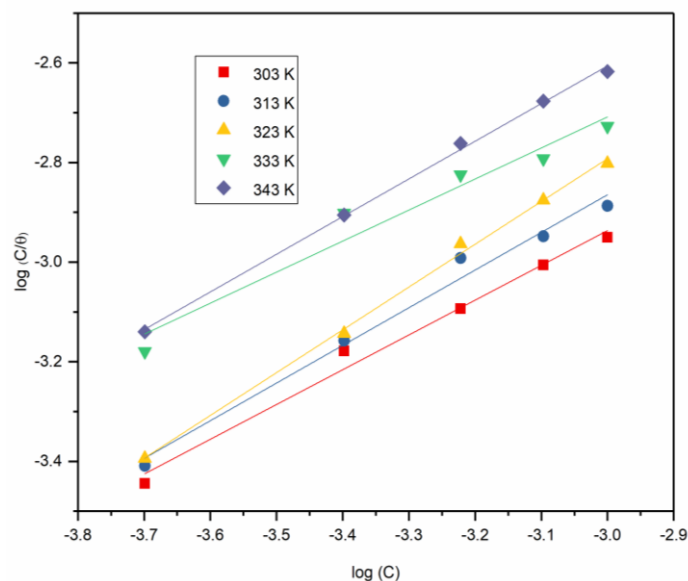


Figure 10. Langmuir isotherm for the adsorption of BPE on carbon steel surface in 1.0 M HCl solution at various temperatures

Table 7. Langmuir parameters for the corrosion of carbon steel in 1.0 HCl containing various concentrations of BPE

T (K)	Slope	Intercept	R ²	k _{ads}	ΔG ⁰ _{ads} (kJ/mol)
303	0.6984	-0.8416	0.9876	0.1440	-5.24
313	0.7563	-0.5959	0.9855	0.2536	-6.88
323	0.8593	-0.2145	0.9975	0.6102	-9.46
333	0.6233	-0.8387	0.9539	0.1450	-5.77
343	0.7564	-0.3369	0.9982	0.4604	-9.24

4.6. FTIR Analysis

Figure 3 shows the infrared spectra of raw BPE and that of BPE adsorbed on the carbon steel surface. Almost all the peaks (**Table 2**) which appeared in the raw extract are no longer visible in the corrosion product. The only visible peak which was strong at 3567.01 in the raw sample became weak in the corrosion product. This is indicative of the fact that atoms contained in BPE have actively participated in the adsorption process, forming metal complexes that are active against corrosion reactions.

4.7. DFT calculations on corrosion inhibition potential of the compound

Quantum chemical calculations were performed to gain insight at the molecular level, electron distribution of the inhibitor as well as to understudy the nature of its interactions with the metal surfaces. CEU, the identified organic compound was examined for possible application as corrosion inhibitor. The 3-dimensional (3D) structure of the compound (**Figure 11**) was retrieved from the PubChem database for chemical molecules [24].

For clearer view of the structures, Chem3D Ultra 10.0 program [25] was used to obtain a 2D version (**Scheme 1**) of the molecules from their 3D formats.

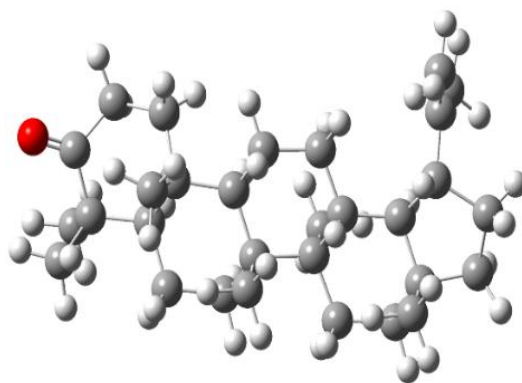
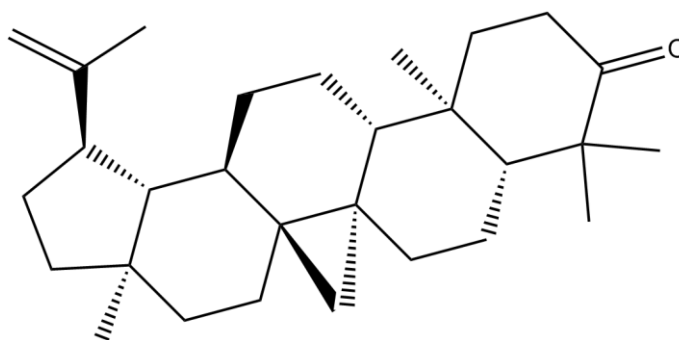


Fig. 11. The 3D structures of CEU



Scheme 1. The 2D diagram of CEU

The Gauss View 6.0 program [26] was employed for calculation set ups and outputs visualization. Widely embraced density functional theory (DFT) model embedded in Gaussian 16 [27] was utilized for all calculations. The hybrid density B3LYP functional [28] in conjunction with the 6-31+G(d,p) basis set was the chosen model for all calculations. The calculations carried out include

geometry optimization, frequency optimization, and ultraviolet-violet (UV-Vis) calculations. Geometry optimization was carried out, first in the gas-phase and then in the experimental solvent, HCl. The optimized geometries of the molecules from geometry optimization were used as the starting structures for the two subsequent calculations.

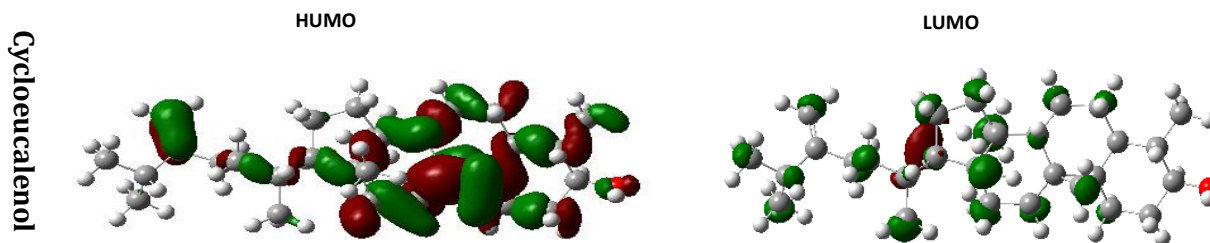


Fig. 12. The HUMO and LUMO density of CEU by using DFT at the B3LYP/6-31G (d,p) Basis Set Level

The frequency optimization involved optimization to a minimum, done for neutral

(zero charge and singlet spin), cationic (+1 charge and doublet spin), and anionic (-1 charge

and doublet spin) molecules of each compound. These afford the determination of the atomic population charges, and then the Fukui function and further assessment of the possible centres of corrosion inhibition. The UV-Vis calculation

Table 7. The electronic properties and global reactivity descriptors for CEU

E_{LUMO} (eV)	E_{HOMO} (eV)	ΔE (eV)	A (eV)	I (eV)	η (eV)	δ (eV ⁻¹)	χ (eV)	C_p (eV)	ω (eV)	ΔN	μ (Debye)
-0.82	-6.54	5.72	6.54	0.82	2.86	0.34	3.68	-3.68	2.37	0.57	4.98

All optimized structures are true local minima with no negative vibration frequency. The molecular orbital energies which include the lowest unoccupied molecular orbital, E_{LUMO} , and the highest occupied molecular orbital, E_{HOMO} (**Figure 12**) were determined from the single-point energy calculation (**Table 7**). A difference of these two parameters gives the energy gap (ΔE). Chemical hardness, η measures the possibility of molecules to bind and interact with other molecules. It is a guiding index to construct the intermolecular reactivity sequence of any given compound or group of compounds, [29]. Low η values were obtained with corresponding the high values of δ for CEU which reflects soft and strong intermolecular reactivity. A ΔN value greater than zero indicates that such molecule will donate electron to any interacting species [30-31]. CEU will donate the appreciable number of electrons, and thus act as good inhibitors because the ΔN are way close to 1, with ΔN values of 0.55 will possess the good inhibitory potential.

In general, CEU consists of three atoms namely oxygen, carbon, and hydrogen. The polarity in CEU could arise from the electronegative carbonyl oxygen atom at a rare end of the molecule relative to the many aliphatic groups in the molecule which makes it a good inhibitor of corrosion.

4.5.2. Molecular Orbital and Fukui Index Analysis

The HOMO map shows electron cloud situated in the C=C sp^2 group, and then spread across the

entails single-point energy calculation for the determination of the molecular orbital energies for further evaluation of the energy gap and other electronic properties.

three consecutive cyclohexane rings and their substituents. From the Fukui function indices calculations, CEU is discovered to have its site for nucleophilic and electrophilic attacks each at one of carbon atoms of the alkene group in the molecule. The results have demonstrated the ability of CUE molecule to protect steel metal surface from corrosion in HCl acidic medium.

5. Conclusion

BPE has proven to be a good inhibitor for the corrosion of carbon steel in HCl. The %IE was found to increase with increase in the inhibitors concentration but decrease with temperature. The gravimetric, electrochemical, and computational results are in a good agreement. The negative values of entropy changes of adsorption (ΔS) implies that the activation complex represents association steps and that the reaction was spontaneous and feasible. The spontaneity was corroborated by the values of ΔG_{ads}^0 . Also, the results showed that all the enthalpy of activation (ΔH) for the inhibitors are negative, reflecting the exothermic nature of the carbon steel dissolution process in HCl. From the value of the activation energy (EA), standard free energy of adsorption ΔG_{ads}^0 , and the adsorption studies, the physically adsorbed BPE on the carbon steel surface in HCl was found to obey Langmuir adsorption isotherm. CEU is discovered to have its site for nucleophilic and electrophilic attacks each at one of carbon atoms of the alkene group in the molecule. Its ability to donate appreciable number of electrons makes it act as a good inhibitor.

Funding

No funding was received for the current work

Conflict of Interests

The authors declare no conflict of interests.

Acknowledgement

The authors extend their appreciation to the Department of Chemistry, University of Agriculture for granting us access to their laboratories and equipment, respectively.

References

- [1] D. Zhang, H. Zhang, S. Zhao, Z. Li, S. Hou, Electrochemical Impedance Spectroscopy Evaluation of Corrosion Protection of X65 Carbon Steel by Halloysite Nanotube-Filled Epoxy Composite Coatings in 3.5% NaCl Solution. *Int. J. Electrochem. Sci.*, 14 (2019) 4659 - 4667.
- [2] B.R. Fazal, T. Becker, B. Kinsella, K. Lepkova, A review of plant extracts as green corrosion inhibitors for CO₂ corrosion of carbon steel. *npj Materials Degradation*, 5 (2022).
- [3] D.C. Benjamin, A.L. Richard, H.R. David, Corrosion control and monitoring; a program management guide for selecting materials. *Advanced Materials, Manufacturing and Testing Information Analysis Center (AMMTIAC), New York, USA*, (2006) 1-19.
- [4] G.A. Ijuo, S. Nguamo, J.O. Igoli, Ag-nanoparticles Mediated by *Lonchocarpus laxiflorus* Stem Bark Extract as Anticorrosion Additive for Mild Steel in 1.0 M HCl Solution. *Prog. Chem. Biochem. Res.*, 5(2022) 133-146.
- [5] A.K. Kuropatnicki, E. Szliszka, W. Krol, Historical aspects of propolis research in modern times. *Evid. Based Complement. Alternat. Med.*, 2013 (2013).
- [6] E.V. Starostensko, Propolization by bees of various races, *Pchelovodstvo*, 88 (1968) 30.
- [7] V.D. Wagh, Propolis, a wonder bee's product and its pharmacological potentials. *Adv Pharmacol Sci.*, 308249 (2013)
- [8] G.A. Burdock, Review of the biological properties and toxicity of bee propolis. *Food and Chemical Toxicology*, 36 (1998) 347-363
- [9] S. Patil, N. Desai, K. Mahadik, A. Paradkar, can green synthesized propolis loaded silver nanoparticulate gel enhance wound healing caused by burns? *European Journal of Integrative Medicine*, S1876-3820 (2015) 00043-8
- [10] H.F.Chahul, C.O. Akalezi, A.M. Ayuba, Effect of adenine, guanine and hypoxanthine on the corrosion of mild steel in H₃PO₄. *International Journal of Chemical Science*, 7 (2015) 2006-3350.
- [11] C.V.S. Prakash, I. Prakash, Isolation and Structural Characterisation of Lupane Triterpenes from *Polypodium Vulgare*, *Research Journal of Pharmaceutical Sciences*. 1 (2012) 23-27
- [12] E.A. Adewusia, P. Steenkamp, G. Fouche, and V. Steenkamp, Isolation of cycloeucalenol from *Boophone disticha* and evaluation of its cytotoxicity, *Natural Product Communications*, 8 (2013) 1213-1216
- [13] N. Bhardwaj, P. Sharma, V. Kumar Phytochemicals as steel corrosion inhibitor: an insight into mechanism *Tenside Surf. Det.*, 59 (2022) 81-94.
- [14] W.A.W. Elyn, Corrosion inhibition of mild steel in 1 M HCl solution by *Xylopiia Ferruginea* leaves from different extract and partitions, *Int. J. Electrochem. Sci.* 6 (2011) 2998-3016.
- [15] G.A. Ijuo, A.M. Orokpo, P.N. Tor, Effect of Spondias mombin Extract on the Corrosion of Mild Steel in Acid Media, *Chemrj*, 3 (2018) 64-77
- [16] E. Ituen, A. Singh, L. Yuanhua, O. Akaranta, Green synthesis and anticorrosion effect of *Allium cepa* peels extract-silver nanoparticles composite in simulated oilfield pickling solution, *SN Appl. Sci.*, 3 (2021) 679.
- [17] N.B. Iroha, N.J. Maduelosi, Corrosion Inhibitive Action and Adsorption Behaviour

- of *Justicia Secunda* Leaves Extract as an Eco-Friendly Inhibitor for Aluminium in Acidic Media, 11 (2021) 13019–13030
- [18] A.I. Ali, Y.S. Mahrousb, Corrosion inhibition of C-steel in acidic media from fruiting bodies of *Melia azedarach* L extract and a synergistic Ni²⁺ additive, *RSC Adv.* 7 (2017) 23687-23698
- [19] N. Al Otaibi, H.H. Hammud, Corrosion Inhibition Using Harmal Leaf Extract as an Eco-Friendly Corrosion Inhibitor, *Molecules*, 26 (2021) 7024.
- [20] O.O. Adeyemiand, O.O. Olubomehin, Investigation of Anthocleista djalonesis stem bark extract of corrosion inhibitor for aluminium. *Pacific J. Sci. Technol.* 11 (2010) 455-462.
- [21] M. Ismail, A.S. Abdulrahman, M.S.Hussain, Solid waste as environmental benign corrosion inhibitors in acid medium. *Int. J. Engg. Sci. Technol.*, 3(2) (2011) 1742-1748.
- [22] E.F. Olasehinde, S.J. Olusegun, A.S. Adesina, S.A. Omogbehin, H. Momoh- Yahayah, Inhibitory action of *Nicotiana tobacum* extracts on the corrosion of mild steel in HCl: adsorption and thermodynamic study, *Natural Science.*, 11 (2013) 83-90
- [23] N. J. Maduelosi and N.B. Iroha, Insight into the Adsorptive Inhibitive effect of Spironolactone Drug on C38 Carbon Steel Corrosion in Hydrochloric Acid Environment. *Journal of Bio and Tribo-Corrosion*, 7 (2021) z.
- [24] N.O. Eddy and A.S. Ekop, Inhibition of corrosion of zinc in 0.1M H₂SO₄ by 5-amino-1-cyclopropyl-7-[(3r,5s) 3, 5-dimethylpiperazin-1-yl]-6,8-difluoro-4-oxoquinolne-3-carboxylic acid, *Material Science AII.*, 4 (2007) 2008-2016.
- [25] S. Kim, P.A. Thiessen, E.E. Bolton, J. Chen, G. Fu, A. Gindulyte, L. Han, J. He, S. He, B.A. Shoemaker, and J. Wang, substance and compound databases. *Nucleic acids research, Pub Chem.*, 44 (2016) D1202-D1213.
- [26] Z.Z.H. Zhenli, The Computation Basis of Software CS Chem3D and its Application in Organic Chemistry, *Guang Zhou Chemical Industry and Technology*, 2 (2002).
- [27] R. Dennington, T.A. Keith, J.M. Millam, GaussView 6.0. 16, Shawnee Mission, 2016.
- [28] M.J. Frisch, G.W. Trucks, H.B. Schlegel, G.E. Scuseria, M.A. Robb, J.R. Cheeseman, G. Scalmani, V. Barone, G.A. Petersson, H. Nakatsuji, X. Li, *Gaussian.*, 16 (2016).
- [29] F.J. Devlin, J.W. Finley, P.J. Stephens, and M.J. Frisch, Ab initio calculation of vibrational absorption and circular dichroism spectra using density functional force fields: a comparison of local, nonlocal, and hybrid density functionals. *The Journal of Physical Chemistry*, 99(1995) 16883-16902.
- [30] R.K. Roy, S. Krishnamurti, P. Geerlings, and S. Pal, Local softness and hardness-based reactivity descriptors for predicting intra-and intermolecular reactivity sequences: carbonyl compounds, *The Journal of Physical Chemistry A*, 102 (1998) 3746-3755.
- [31] I.B. Obot, D.D. Macdonald, and Z.M. Gasem, Density functional theory (DFT) as a powerful tool for designing new organic corrosion inhibitors. Part 1: an overview. *Corrosion Science*, 99 (2015) 1-30.

HOW TO CITE THIS ARTICLE

A. M. Orokpo, R. A. Wuana, H.F. Chuhul, I.S. Eneji. Corrosion Inhibition Potentials of Benue Propolis Extracts on Carbon Steel in 1.0 M Hydrochloric Acid Medium: Experimental and Computational Studies. *Prog. Chem. Biochem. Res.* 5(3) (2022) 283-300.

DOI: 10.22034/pcbr.2022.354920.1231

URL: http://www.pcbiochemres.com/article_158138.html

